

# Modeling control and simulation of two axes gimbal seeker using fuzzy PID controller

Maher Abdo  
PhD student  
Electrical Engineering  
Malek Ashter University  
Tehran, Iran  
maherabdo74@yahoo.com

Ahmad Reza Vali  
Assistant Professor  
Electrical Engineering  
Malek Ashter University  
Tehran, Iran  
Ar.vali@aut.ac.ir

Ali Reza Toloei  
Assistant Professor  
Aerospace Department  
Shahid Beheshti University  
Tehran, Iran  
toloei@sbu.ac.ir

Mohammad Reza Arvan  
Assistant Professor  
Electrical Engineering  
Malek Ashter University  
Tehran, Iran  
m\_r\_arvan@yahoo.com

**Abstract**— The application of the guided missile seeker is to provide stability to the sensor by isolating it from the missile motion and vibration. The aim of this paper is to present the model of two axes gimbal seeker and improve its performance using proposed fuzzy controller. The equations of gimbals motion are derived using Lagrange equation and the stabilization system is constructed considering the missile rates, torque disturbances, and cross coupling between elevation and azimuth channels. The overall control system is simulated using MATLAB/Simulink. This model is evaluated comparing with conventional PI control system. The comparative simulation results in different conditions have shown that the proposed fuzzy PID method offers a better performance than the classical one.

**Keywords**—line of sight; gimbal seeker; rate gyro; guided missile; servo tracking loop

## I. INTRODUCTION

The seeker is the part of guided missile which deals with the target throughout detection phase where it must detect a target rapidly in a large search area, then tracking phase which must be made accurately to perform the interception between missile and target at the end of engagement. Gimballed seekers have found wide applications in modern advanced tactical homing missiles. They are used to track the target and to provide the inertial stabilization to the detector's (sensor) pointing vector [1]. In order to keep the sensor stable despite of disturbances, a two axes gimbal system is used so that the sensor is located on the inner gimbal. Most disturbances result from missile motions, gimbal system geometry, and gimbal system imperfections like mass unbalance. Therefore, the dynamics of the plant must be expressed in analytical form before the design of gimbal system is taken up. The mathematical model and control system of two axes gimbal system have been investigated in many researches utilizing different forms. Concerning the mathematical model, several derivations have been proposed using different assumptions. Reference [2] has presented the kinematics and geometrical coupling relationships for two degree of freedom gimbal assembly for a simplified case when each gimbal is balanced. In [3], Ekstrand has derived the equations of motion for the two

axes gimbal configuration assuming that the gimbals have no mass imbalance and inertia disturbances and cross couplings can be eliminated by certain inertia symmetry conditions. For one degree of freedom gimbal studied in [4], the static and dynamic imbalance disturbance torques created by the vibrations of operating environment can be eliminated by statically and dynamically balancing the gimbal, which is regarded costly and time consuming. In [5], the motion equations of two axes gimbal system have been derived assuming that gimbals have no dynamic mass imbalance and the effects of base rates were not highlighted. The research in [6] has introduced a two axes gimbal mechanism where just the modeling of azimuth axis was focused, while the elevation angle was kept fixed and cross moments of inertia were taken to be zero. Also, in [7], the dynamical models of elevation and azimuth gimbals have been derived assuming that the products of inertia can be neglected. In above researches, the model of two axes gimbal system was derived using Newtonian approach. Also, the gimbal system model has been often simplified using different approaches such as, disregarding the connection between gimbals then applying the study on one gimbal, by taking into account that disturbances result from system imperfections can be ignored utilizing some assumptions. In addition, the gimbal systems designed in such a researches were not tested and evaluated under the operating conditions affected the base on which the gimbal system is located. On the other hand, the control system of two axes gimbal configuration has been constructed using different control approaches. Proxy-based sliding mode has been applied in [5]. Reference [8] proposed the sliding mode control under the assumption of uncoupled identical elevation and azimuth channels. Modern synthesis tools such as linear quadratic regulator or linear quadratic Gaussian with loop transfer recovery control for a wideband controller have been used in (LOS) stabilization in [9]. Besides these conventional control methods, some advance control techniques, such as fuzzy logical control [10], robust control [11], variable structure control [12], and  $H_\infty$  control methodology [13]. However, a majority of these algorithms were complex and difficult to be realized. In recent years, the fuzzy control technology has been developed successfully. It improves the

system control performance, and has the good adaptability for the system with nonlinear mathematical model and uncertain factors [14]. Therefore, this paper is devoted to introduce fuzzy PID technique for two axes gimbal seeker of guided missile. The paper is organized as follows. Second section formulates the problem. In third section, the motion equations are derived using Lagrange equation considering the cross coupling which results from the gimbals geometry and missile angular motion. Also, the torque disturbance of dynamic unbalance is concerned because even in a well designed gimbal systems this defect is inevitable. The stabilization loop and proposed controller are designed in fourth and fifth sections respectively. The control aims are mainly to achieve good transient and steady-state performance with respect to step input commands. Seventh section presents simulation results, and finally conclusion remarks are highlighted.

## II. PROBLEM FORMULATION

A target seeker attempts to align its detector axis in elevation and azimuth with a line of sight (LOS) joining the seeker and target. The seeker contains two loops: outer track loop, and inner stabilizing loop AS SHOWN IN Fig. 1.

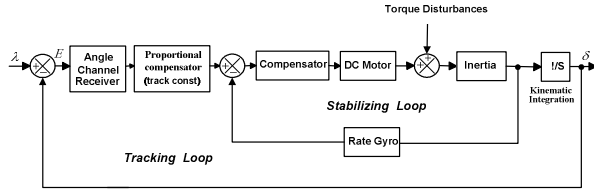


Figure 1. One axis seeker

Based on the information received by the sensor, the track loop generates a rate commands to direct gimbal boresight toward the target LOS, and to maintain the measured boresight error near zero, while the stabilization loop isolates the sensor placed on the elevation gimbal from missile motion and disturbances that would otherwise perturb the aim-point. In this way the control system is formulated so that the inner gimbal is successfully isolated from disturbances and missile vibrations, and the sensor optical axis is kept nonrotating and its direction is maintained in inertial space despite disturbances. Fig. 2 shows how the missile seeker works. Where  $\lambda$  is LOS angle,  $\delta$  is boresight angle, and  $E$  is boresight error angle or pointing error.

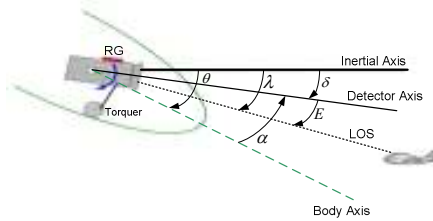


Figure 2. Missile seeker angular geometry

The two control loops in elevation and azimuth channels are related by the cross coupling unit which is built based on the torques relationships. The cross coupling express the properties of the gimbal system dynamics. It reflects the fact that the azimuth gimbal can affect on the elevation gimbal even when the base (missile body) is non-rotating. Also, there is similar impact from the elevation gimbal on the azimuth gimbal. As a result, the cross coupling may be defined as the effect on one axis by the rotation of another [4].

## III. EQUATIONS OF GIMBALS MOTION

In this paper, a two axes gimbal system depicted in Fig. 3 is considered. The sensor is placed on the elevation gimbal. Three reference frames are identified as follows:  $P$  frame fixed to the fuselage body with axes  $(i, j, k)$ ,  $B$  frame fixed to the azimuth (outer) gimbal with axes  $(n, e, k)$ , and  $A$  frame fixed to the elevation (inner) gimbal with axes  $(r, e, d)$ .

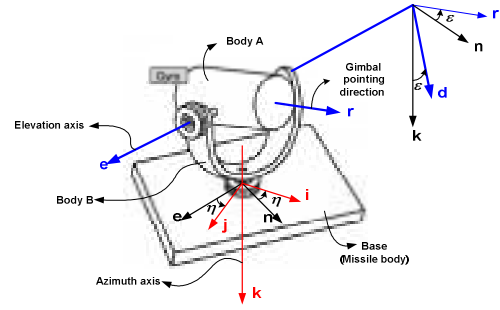


Figure 3. Two axes gimbal system

The  $r$ -axis coincides with the sensor optical axis. Using rotation angles  $\epsilon$  and  $\eta$ , the transformation matrices are given by

$${}^B_P C = \begin{bmatrix} \cos \eta & \sin \eta & 0 \\ -\sin \eta & \cos \eta & 0 \\ 0 & 0 & 1 \end{bmatrix}, {}^A_B C = \begin{bmatrix} \cos \epsilon & 0 & -\sin \epsilon \\ 0 & 1 & 0 \\ \sin \epsilon & 0 & \cos \epsilon \end{bmatrix} \quad (1)$$

Where  ${}^B_P C$  and  ${}^A_B C$  are the transformation from  $P$  frame to  $B$  frame and the transformation from  $B$  frame to  $A$  frame respectively. The inertial angular velocity vectors of frames  $P$ ,  $B$ , and  $A$ , respectively are

$${}^P \bar{\omega}_{P/I} = \begin{bmatrix} \omega_{pi} \\ \omega_{pj} \\ \omega_{pk} \end{bmatrix}, {}^B \bar{\omega}_{B/I} = \begin{bmatrix} \omega_{Bn} \\ \omega_{Be} \\ \omega_{Bk} \end{bmatrix}, {}^A \bar{\omega}_{A/I} = \begin{bmatrix} \omega_{Ar} \\ \omega_{Ae} \\ \omega_{Ad} \end{bmatrix} \quad (2)$$

Where  $\omega_{pi}, \omega_{pj}, \omega_{pk}$  are the missile body angular velocities of frame  $P$  in relation to inertial space about  $i, j$ , and  $k$  axes respectively,  $\omega_{Bn}, \omega_{Be}, \omega_{Bk}$  are the azimuth gimbal angular velocities in relation to inertial space about  $n, e$ , and  $k$  axes respectively, and  $\omega_{Ar}, \omega_{Ae}, \omega_{Ad}$  are the elevation gimbal angular velocities in relation to inertial space about the  $r, e$ , and  $d$  axes respectively. Inertia matrices of the elevation and azimuth gimbals respectively are

$${}^A J_{inner} = \begin{bmatrix} A_r & A_{re} & A_{rd} \\ A_{re} & A_e & A_{de} \\ A_{rd} & A_{de} & A_d \end{bmatrix}, {}^B J_{outer} = \begin{bmatrix} B_n & B_{ne} & B_{nk} \\ B_{ne} & B_e & B_{ke} \\ B_{nk} & B_{ke} & B_k \end{bmatrix} \quad (3)$$

Where  $A_r, A_e, A_d$  are elevation gimbal moments of inertia about r, e, and d axes,  $A_{re}, A_{rd}, A_{de}$  are elevation gimbal moments products of inertia,  $B_n, B_e, B_k$  are azimuth gimbal moments of inertia about n, e, and k axes, and  $B_{ne}, B_{nk}, B_{ke}$  are azimuth gimbal moments products of inertia. Also, it is introduced  $T_{EL}$  and  $T_{AZ}$  as the total external torques about elevation gimbal e-axis and azimuth gimbal k-axis respectively. The aim is to stabilize the gimbal system LOS (r-axis), that means the outputs rates  $\omega_{Ae}$  and  $\omega_{Ad}$  must be equal to zero so the sensor is kept non-rotating in inertial space despite disturbances.  $\omega_{Ae}, \omega_{Ad}$  can be measured by a rate gyro placed on the elevation gimbal. In general, Euler angles define the position between two related reference frames. For the body fixed frame P and azimuth gimbal frame B with one angle  $\eta$ , we have

$$\begin{aligned} \omega_{Bn} &= \omega_{pi} \cos \eta + \omega_{pj} \sin \eta & (a) \\ \omega_{Be} &= -\omega_{pi} \sin \eta + \omega_{pj} \cos \eta & (b) \\ \omega_{Bk} &= \omega_{pk} + \dot{\eta} & (c) \end{aligned} \quad (4)$$

Similarly, between azimuth gimbal frame B and elevation gimbal A frame we have

$$\begin{aligned} \omega_{Ar} &= \omega_{Bn} \cos \varepsilon - \omega_{Bk} \sin \varepsilon & (a) \\ \omega_{Ae} &= \omega_{Be} + \dot{\varepsilon} & (b) \\ \omega_{Ad} &= \omega_{Bn} \sin \varepsilon + \omega_{Bk} \cos \varepsilon & (c) \end{aligned} \quad (5)$$

The orientation of the gimbal system in an inertial system is completely determined by four independent consecutive rotations  $\phi, \theta, \psi, \varepsilon$  where  $\phi, \theta, \psi$  are the three Euler rotations of the azimuth gimbal and  $\varepsilon$  is the elevation gimbal angle [3]. By taking the rotations in the order roll  $\phi$ , elevation  $\theta$ , and azimuth  $\psi$  followed by  $\varepsilon$ , the generalized “forces” corresponding to the coordinates  $\psi$  and  $\varepsilon$  are the external torques  $T_{AZ}$  and  $T_{EL}$  applied to the azimuth and elevation gimbals, respectively [3]. Therefore, the azimuth gimbal angular velocities can be also derived as follows

$$\begin{aligned} \omega_{Bn} &= \dot{\phi} \cos \theta \cos \psi + \dot{\theta} \sin \psi \\ \omega_{Be} &= -\dot{\phi} \cos \theta \sin \psi + \dot{\theta} \cos \psi \\ \omega_{Bk} &= \dot{\phi} \sin \theta + \dot{\psi} \end{aligned} \quad (6)$$

The kinetic energy of a rotating body is given by the scalar product [3] indicated by  $T$  as follow

$$T = \bar{\omega} \cdot \frac{\bar{H}}{2}; \bar{H} = J \bar{\omega} \quad (7)$$

Where  $\bar{H}$  is the angular momentum,  $\bar{\omega}$  is the inertial angular velocity of the body expressed in the body fixed frame, and  $J$  is the inertia matrix of the body. Thus, using (2) and (3), the total kinetic energy of two axes gimbal system is given by the sum of kinetic energy of elevation and azimuth gimbals.

$$\begin{aligned} T &= \bar{\omega} \cdot \frac{\bar{H}}{2} \Big|_A + \bar{\omega} \cdot \frac{\bar{H}}{2} \Big|_B = \frac{1}{2} (A_r \omega_{Ar}^2 + A_e \omega_{Ae}^2 + A_d \omega_{Ad}^2) \\ &+ A_{re} \omega_{Ar} \omega_{Ae} + \frac{1}{2} (B_n \omega_{Bn}^2 + B_e \omega_{Be}^2 + B_k \omega_{Bk}^2) + B_{ne} \omega_{Bn} \omega_{Be} \\ &+ A_{rd} \omega_{Ar} \omega_{Ad} + A_{de} \omega_{Ae} \omega_{Ad} + B_{nk} \omega_{Bn} \omega_{Bk} + B_{ke} \omega_{Be} \omega_{Bk} \end{aligned} \quad (8)$$

Inserting (6) and (5) in (8) gives the kinetic energy as a function of the generalized coordinates and their time derivatives. Then, Lagrange equation can be formulated and equations of motion obtained. Concerning the azimuth gimbal, The Lagrange equation for  $\psi$  is

$$\frac{d}{dt} \left( \frac{\partial T}{\partial \dot{\psi}} \right) - \frac{\partial T}{\partial \psi} = T_{AZ} \quad (9)$$

Where  $T$  is the kinetic energy given in (8). The equation of azimuth gimbal motion can be derived as a differential equation for  $\omega_{Ad}$  as follows

$$\begin{aligned} J_{eq} \dot{\omega}_{Ad} &= T_{Az} \cos \varepsilon + (T_{d1} + T_{d2} + T_{d3}) \cos \varepsilon + T'_d \\ ; J_{eq} &= B_k + A_r \sin^2 \varepsilon + A_d \cos^2 \varepsilon - A_{rd} \sin(2\varepsilon) \\ ; T'_d &= J_{eq} [\dot{\omega}_{Bn} \sin \varepsilon + \omega_{Ar} (\omega_{Ae} - \omega_{Be})] \\ ; T_{d1} &= \left[ \begin{aligned} &B_n + A_r \cos^2 \varepsilon + A_d \sin^2 \varepsilon \\ &+ A_{rd} \sin(2\varepsilon) - (B_e + A_e) \end{aligned} \right] \omega_{Bn} \omega_{Be} \\ ; T_{d2} &= - \left[ \begin{aligned} &B_{nk} + (A_d - A_r) \sin \varepsilon \cos \varepsilon \\ &+ A_{rd} \cos(2\varepsilon) \end{aligned} \right] (\dot{\omega}_{Bn} - \omega_{Be} \omega_{Bk}) \\ &- (B_{ke} + A_{de} \cos \varepsilon - A_{re} \sin \varepsilon) (\dot{\omega}_{Be} + \omega_{Bn} \omega_{Bk}) \\ &- (B_{ne} + A_{re} \cos \varepsilon + A_{de} \sin \varepsilon) (\omega_{Bn}^2 - \omega_{Be}^2) \\ ; T_{d3} &= \dot{\varepsilon} [(A_r - A_d) (\omega_{Bn} \cos(2\varepsilon) - \omega_{Bk} \sin(2\varepsilon))] \\ &+ \dot{\varepsilon} [(A_{de} \sin \varepsilon + A_{re} \cos \varepsilon) (\omega_{Ae} + \omega_{Be}) - A_e \omega_{Bn}] \\ &+ \dot{\varepsilon} [2 A_{re} (\omega_{Bn} \sin(2\varepsilon) + \omega_{Bk} \cos(2\varepsilon))] \\ &+ \dot{\varepsilon} (A_{re} \sin \varepsilon - A_{de} \cos \varepsilon) \end{aligned} \quad (10)$$

Where  $J_{eq}$  is the instantaneous moment of inertia about k-axis. The disturbances affected on azimuth gimbal are denoted by

$$T_{D-AZ} = (T_{d1} + T_{d2} + T_{d3}) \cos \varepsilon + T'_d \quad (11)$$

For elevation gimbal, Lagrange equation for  $\varepsilon$  is

$$\frac{d}{dt} \left( \frac{\partial T}{\partial \dot{\varepsilon}} \right) - \frac{\partial T}{\partial \varepsilon} = T_{EL} \quad (12)$$

The elevation gimbal motion equation is obtained as a differential equation for  $\omega_{Ae}$  as follows

$$\begin{aligned} A_e \dot{\omega}_{Ae} &= T_{EL} + (A_d - A_r) \omega_{Ar} \omega_{Ad} + A_{rd} (\omega_{Ar}^2 - \omega_{Ad}^2) \\ &- A_{de} (\dot{\omega}_{Ad} - \omega_{Ae} \omega_{Ar}) - A_{re} (\dot{\omega}_{Ar} + \omega_{Ae} \omega_{Ad}) \end{aligned} \quad (13)$$

The disturbances affected on elevation gimbal are denoted by

$$\begin{aligned} T_{D-EL} &= (A_d - A_r) \omega_{Ar} \omega_{Ad} + A_{rd} (\omega_{Ar}^2 - \omega_{Ad}^2) \\ &- A_{de} (\dot{\omega}_{Ad} - \omega_{Ae} \omega_{Ar}) - A_{re} (\dot{\omega}_{Ar} + \omega_{Ae} \omega_{Ad}) \end{aligned} \quad (14)$$

The dynamic mass imbalance is the result of a non-symmetrical mass distribution called Product of Inertia [4]. The dynamic mass imbalance concept can be indicated by the

inertia matrix. When the gimbal has a symmetrical mass distribution with respect to its frame axes, then it has no dynamic mass imbalance and its inertia matrix is diagonal and vice versa. In this paper, the motion equations have been derived assuming that both gimbals have dynamic mass imbalance.

#### IV. SEEKER STABILIZATION LOOP CONSTRUCTION

It can be seen from Fig. 1 that the stabilization loop is constituted of controller, DC motor, platform, and rate gyro. In this paper, the 475T rate gyro from US Dynamics Company is used. Assuming that the gyro natural frequency is 50 Hz, and the damping ratio is 0.7, the gyro transfer function is

$$G_{Gyro}(s) = \frac{\omega_n^2}{(s^2 + 2\zeta\omega_n s + \omega_n^2)} = \frac{2500}{(s^2 + 70s + 2500)} \quad (15)$$

The platform represents the motor load, which is attached to the output of the gears or directly to the shaft motor. The platform is modelled based on its moment of inertia  $J$  that depends on its dimensions and its position respect to the axis of rotation. In this paper, a disc is proposed to represent the platform where its mass  $M = 1 \text{ kg}$  and radius  $r = 14 \text{ cm}$ . Thus,

its moment of inertia is  $J = \frac{1}{2}Mr^2 = 9.8 \times 10^{-3} \text{ Kg.m}^2$ . DC motor from the NORTHROP GRUMMAN Company is utilized. The specifications of this DC motor are: nominal voltage  $u_a = 27 \text{ V}$ , terminal resistance  $R_a = 4.5 \Omega$ , terminal inductance  $L_a = 0.003 \text{ H}$ , rotor inertia  $J_m = 0.0017 \text{ Kg.m}^2$ , torque constant  $K_{TM} = 0.85 \text{ Nm/A}$ , back EMF  $K_e = 0.85 \text{ V/rad/sec}$ , and damping ratio  $a_m = 0$ . Therefore, the transfer function of DC motor can be indicated as follows

$$G_m(s) = \frac{\omega_m(s)}{u_a(s)} = \frac{K_{TM}}{(L_a s + R_a) \cdot (J_m^* s + a_m^*) + K_e K_{TM}} \quad (16)$$

$$= \frac{24637.68}{s^2 + 1500s + 20942}; J_m^* = J_m + J_L, a_m^* = a_m + a_L$$

Where  $J_L$  represents the load inertia which will be computed next,  $a_L$  is the load damping ratio which is supposed to be zero, and  $\omega_m(s)$  is the motor's angular velocity. In order to evaluate the efficiency of proposed fuzzy controller, two PI controllers  $K_{EL}(s)$  and  $K_{AZ}(s)$  are defined utilizing trail and error approach to be compared later with the proposed controller.

$$K_{EL}(s) = 0.09 + \frac{12.5}{s}, K_{AZ}(s) = 0.5 + \frac{12.5}{s} \quad (17)$$

#### V. DESIGN OF PROPOSED FUZZY CONTROLLER

The drawback of the conventional PI appears when the control system works under variable conditions. Therefore, in inertia stabilization system proposed, PI controller can not maintain the good performance unless the controller parameters are retuned. The progress report [15] pointed out that the adaptive control technique is the future development direction of LOS inertia stabilization systems. Recent years, fuzzy logic control has been increasingly developed. Basically,

fuzzy controller comprises of four main components as shown in Fig. 4; fuzzification interface, knowledge base, inference mechanism and defuzzification interface.

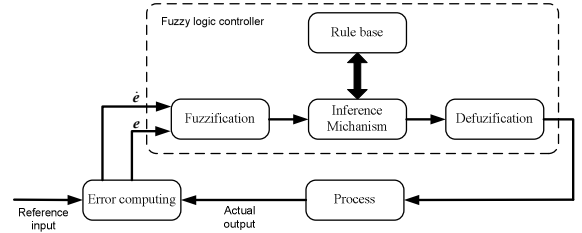


Figure 4. Fuzzy logic controller

One triple-outcome fuzzy controller shown in Fig. 5 is proposed to update the PID parameters ( $K_p, K_i, K_d$ ) online, then provide control signal  $u_c$  with changing conditions.

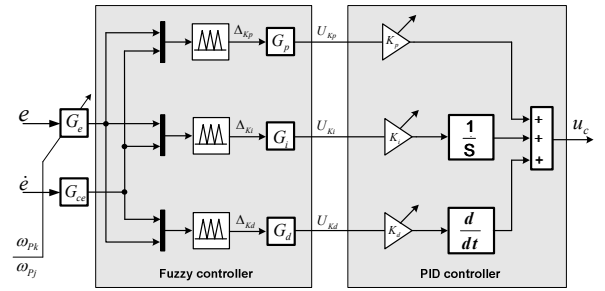


Figure 5. Proposed fuzzy PID type controller

This fuzzy controller can be classified as double input direct action type. This structure uses the error  $e$  and the change of error  $\dot{e}$  as inputs and has three outputs  $\Delta K_p, \Delta K_i, \Delta K_d$ . While  $G_e, G_{ce}$  and  $G_p, G_i, G_d$  represent inputs and outputs scaling factors respectively.  $U_{Kp}, U_{Ki}, U_{Kd}$  are fuzzy control signals. Fig. 6 shows the membership functions (defined on discourse  $[-3, 3]$ ) of input and output variables.

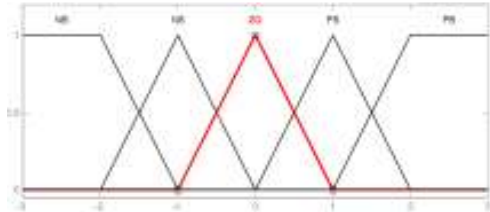


Figure 6. Membership functions

For the membership functions used, NL, NS, ZR, PS, PL denotes negative large, negative small, zero, positive small, and positive large, respectively. The outputs are determined using gravity center method. The PID parameters have a great influence on the stable and dynamic performance of controller

system. The steady-state error reduces as  $K_p$  increases. But when  $K_p$  gets too large, the overshoot is so great and the steady-state is damaged. The climb speed goes faster as  $K_i$  increases. But if  $K_i$  gets too large, it will affect the steady-state operation by causing torque ripples and a serious overshoot. The reduction of  $K_d$  will increase the climb speed and reduce the torque ripple. But if it gets too small, the system will suffer from an overshoot and a long settling time. In order to achieve the control goal, the above knowledge is translated into IF-THEN rule statements indicated in Table I.

TABLE I. RULE BASES

$\Delta_{Kp}$ $\Delta_{Ki}$ $\Delta_{Kd}$		$\dot{e}$				
		NL	NS	ZR	PS	PL
$e$	NL	PL	PS	PS	PS	ZR
		NL	NS	NS	NS	ZR
	NS	PL	PS	PS	ZR	NS
		NL	NS	NS	ZR	PS
	ZR	PS	PS	ZR	NS	NS
		NS	NS	ZR	PS	PS
	PS	PS	ZR	NS	NS	NL
		NS	ZR	PS	PS	PL
	PL	ZR	NS	NS	PS	NL
		ZR	PS	PS	PS	PL

The design parameters of fuzzy PID controllers are summarized within two groups: Structural parameters which are determined during off-line design, and tuning parameters including scaling factors and parameters of membership functions. The selection of tuning parameters is a critical task, which is usually carried out through trial and error or using some training data. Also, these parameters can be calculated during on-line adjustments of the controller to enhance the process performance, as well as to accommodate the adaptive capability to system uncertainty and process disturbance. The fuzzy controller is regarded adaptive if any one of its tunable parameters changes when the controller is being used; otherwise it is conventional fuzzy controller. An adaptive fuzzy controller is named self-tuning if either its scaling factors or membership functions or, both of them are modified. When a fuzzy controller is tuned by automatically changing its rules then it is called a self-organizing fuzzy controller. Scaling factors have the highest priority due to their global effect on the control performance. The most dominant parameters in the performance of two axes gimbal seeker are the missile body rates  $\omega_{pj}$ ,  $\omega_{pk}$ . Therefore, the proposed controller is built as self-tuning fuzzy controller which is tuned online by modifying  $G_e$  based on  $\omega_{pj}$  and  $\omega_{pk}$ . Tuning operation is made utilizing (18) and (19) obtained from parametric study applied on elevation and azimuth channels, respectively.

$$G_e(\omega_{pj}) = -0.0571\omega_{pj}^2 + 0.3192\omega_{pj} + 5.421 \quad (18)$$

$$G_e(\omega_{pk}) = -0.0212\omega_{pk}^2 + 0.076\omega_{pk} + 3.7995 \quad (19)$$

The other tuning parameters are adjusted off-line (as indicated in Table II) based on the knowledge about the process error to achieve the best possible control performance.

TABLE II. OFF-LINE ADJUSTED PARAMETERS

Parameter	$G_{ce}$	$G_p$	$G_i$	$G_d$
Elevation	0.1	0.02	2	0.0001
Azimuth	0.13	0.01	3.5	0.0001

## VI. SIMULATION RESULTS

The overall simulation model is prepared in MATLAB/Simulink environment as depicted in Fig. 7.

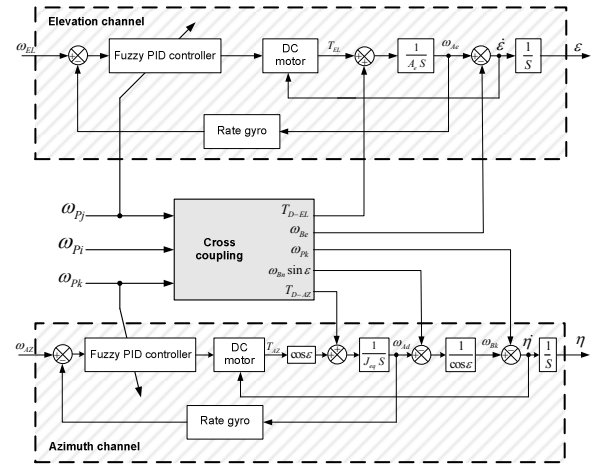
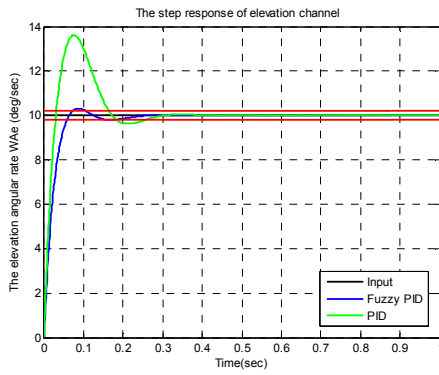
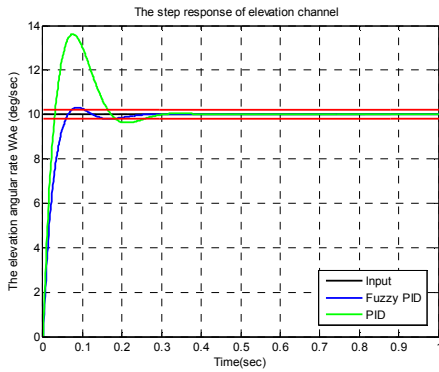


Figure 7. Two axes stabilization loop of gimbal seeker

A comparison of proposed fuzzy controller and conventional PI (17) is carried out using rate input commands in elevation and azimuth channels  $\omega_{ej} = \omega_{ez} = 10 \text{ deg/sec}$ , and rates  $\omega_{pj}$ ,  $\omega_{pk}$  are changed along the interval  $[0-14] \text{ deg/sec}$ . As an example, one case of system response is displayed in Fig. 8 which reflects clearly the efficiency of the fuzzy PID controller compared to the conventional PI. To confirm this efficiency, many comparison tests indicated in Table III and Table V are made utilizing the maximum overshoot (ov), settling time  $t_s$ , and rise time  $t_r$ . Tables III, IV show that when conventional PI is used, the angular rate increment creates large overshoot and increases settling time. While fuzzy PID controller can meet the variation of missile body rates and improves the transient and steady-state performance by achieving fast response with lower overshoot as compared to conventional PI.



(a) Elevation channel



(a) Azimuth channel

Figure 8. Gimbal system response for  $\omega_{pj} = \omega_{pk} = 8 \text{ deg/sec}$

TABLE III. COMPARISON RESULTS OF ELEVATION CHANNEL

$\omega_{pj}$ (deg/sec)	PI controller			Fuzzy PID controller		
	ov (%)	$t_s$ (sec)	$t_r$ (sec)	ov (%)	$t_s$ (sec)	$t_r$ (sec)
2	9.7	0.185	0.06	0	0.132	0.092
4	15.1	0.174	0.042	2	0.112	0.081
6	24.2	0.165	0.032	2.1	0.086	0.062
8	36.2	0.255	0.023	3.2	0.105	0.042
10	50	0.266	0.016	9.2	0.116	0.028

TABLE IV. COMPARISON RESULTS OF AZIMUTH CHANNEL

$\omega_{pj}$ (deg/sec)	PI controller			Fuzzy PID controller		
	ov (%)	$t_s$ (sec)	$t_r$ (sec)	ov (%)	$t_s$ (sec)	$t_r$ (sec)
2	6.7	0.158	0.053	2	0.149	0.102
4	15.2	0.169	0.039	2.1	0.126	0.09
6	25	0.176	0.03	2.2	0.107	0.074
8	35.8	0.188	0.025	2	0.086	0.064
10	47.1	0.2	0.02	3.7	0.123	0.05

## VII. CONCLUSION

In this paper, the two axes gimbal seeker of a guided missile was introduced. The equations of gimbals motion were

derived utilizing Lagrange equation. Afterwards, the complete control system was built considering missile rates, torque disturbances, and cross coupling between channels. A self tuning fuzzy PID controller was proposed. The comparative study results have proved that the fuzzy controller is simply on-line tuned based on the base rates that can be usually measured by inertia measurements unit (IMU). Therefore, the proposed controller is completely applicable unlike to most of adaptive controllers which frequently tuned based on complex algorithms. Also, the proposed controller has considerably reduced the response overshoot without significant increase in the rise time unlike to most of researches in which the overshoot is usually reduced at the expense of rise time value.

## REFERENCES

- [1] S. Yu, and Y. Z. Zhao, "Simulation study on a friction compensation method for the inertial platform based on the disturbance observer," J Aerospace Eng, vol. 222, 2008, pp. 341-346.
- [2] A. Rue, "Precision Stabilization Systems," IEEE Transactions on Aerospace and Electronic Systems, vol. AES-10, 1974, pp. 34-42.
- [3] B. Ekstrand, "Equation of Motion for a Two Axes Gimbal System," IEEE Trans. On Aerospace and Electronic Systems, vol. 37, 2001, pp. 1083-1091.
- [4] R. Daniel, "Mass properties factors in achieving stable imagery from a gimbal mounted camera," Published in SPIE Airborne Intelligence, Surveillance, Reconnaissance (ISR) Systems and Applications V, vol. 6946, 2008.
- [5] H. Özgür, E. Aydan, and E. İsmet, "Proxy-Based Sliding Mode Stabilization of a Two-Axis Gimballed Platform," Proceedings of the World Congress on Engineering and Computer Science, San Francisco, USA, vol. I, 2011.
- [6] S. Ravindra, "Modeling and Simulation of the Dynamics of a Large Size Stabilized Gimbal Platform Assembly," Asian International Journal of Science and Technology in Production and Manufacturing, vol. 1, 2008, pp. 111-119.
- [7] H. Khodadadi, "Robust control and modeling a 2-DOF Inertial Stabilized Platform," International Conference on Electrical, Control and Computer Engineering, Pahang, Malaysia, June 21-22, 2011.
- [8] B. Smith, W. Schrenck, W. Gass, and Y. Shtessel, "Sliding mode control in a two axis gimbal system," IEEE Aerospace Applicat. Conf, vol. 5, 1999, pp. 457-470.
- [9] J. William, and P. Steven, "Optimal motion stabilization control of an electrooptical sight system," Proc. SPIE Conference, vol. 1111, 1989, pp. 116-120.
- [10] J. Moorthy, M. Rajeev, and B. Hari, "Fuzzy controller for line of sight stabilization system," Optical Engineering, vol. 43, 2004, pp. 1394-1400.
- [11] C. Lin, C. Hsu, and Y. Mon, "Self-organizing fuzzy learning CLOS guidance law design," IEEE Trans. AES, vol. 39, 2003, pp. 1144-1151.
- [12] K. Tam, T. Lee, A. Mamum, M. Lee, and C. Khoh "Composit control of a gyro mirror line of sight stabilization platform design and auto tuning," ISA transaction, vol. 40, 2001, pp.155-171.
- [13] J. Moorthy, M. Rajeev, and V. Sule "H $\infty$  control law for line-of-sight stabilization for mobile land vehicles," Optical Engineering, vol. 41, 2002, pp. 2935-2944.
- [14] C. Li, and W. Jing, "Fuzzy PID controller for 2D differential geometric guidance and control problem," IET Control Theory & Applications, vol. 1, 2007, pp. 564-571.
- [15] J. Hilkert, and D. Hullender, "Adaptive control system techniques applied to inertial stabilization systems," Proc. SPIE Conference, vol. 1304, 1990, pp. 190-206.